Universal Journal of Mechanical Engineering 8(2): 84-91, 2020 http://www.hrpub.org
DOI: 10.13189/ujme.2020.080202

Thermal and Hydrodynamic Characteristics of Graphite-H_2O and CuO-H_2O Nanofluids in Microchannel Heat Sinks

Mohammed Abdulqader Sulaiman, Ahmed Mohammed Adham*, Sirwan Farooq Omar

Department of Mechanical and Energy Engineering, Erbil Technical Engineering College, Erbil Polytechnic University, Iraq

Received December 4, 2019; Revised January 8, 2020; Accepted February 7, 2020

Abstract In this study, nanofluids were used as coolant for high-heat dissipation electronic devices with nanoparticle volume concentrations from 1% to 5%. The results were compared to other conventional cooling systems. Graphite-H_2O and CuO-H_2O nanofluids were analyzed at inlet velocities of 0.1 m/s and 1.5 m/s in a rectangular copper shaped microchannel heat sink MCHS with a bottom size of 20mm×20mm. The results indicate that suspended nanoparticles significantly increase thermal conductivity, heat flux, pumping power, and pressure drop. For graphite-water and CuO-water nanofluids at 0.1m/s with 5.0% volume, the greatest percentage increase in thermal conductivity was 15.52% and 14.34%, respectively. Graphite-water at 0.1 m/s and 1.5 m/s with 5% volume fraction had a maximum heat flux of 18% and 3.46%, respectively. CuO-water at 0.1 m/s and 1.5 m/s inlet velocity with the same volume concentrations had a heat flux of 17.83% and 3.33%, respectively. For graphite-H_2O and CuO-H_2O at 0.1 m/s with 5% volume fraction, pumping power and pressure drop were 0.000695 W and 92.63 Pa, respectively. For inlet velocity of 1.5 m/s with same volume concentration were 0.156306 W and 1389.39 Pa, respectively.

Keywords Heat Flux, Minichannel Heat Sink, Nanofluid, Pumping Power, Thermal Conductivity

1. Introduction

Nanofluids, so named by Argonne National Laboratory, are nanoparticle suspensions in a base fluid. Water, engine oil, and ethylene glycol are base fluids with low thermal conductivity. Nanometer-sized particles have higher thermal conductivity than base fluids. Increasing the nanoparticles in a base fluid, even if the volume concentration is low, significantly increases thermal performance [1]. Choi was the first person to use the term "nanofluids". Nanofluid technology a mixture of liquid-solids in which metallic or nonmetallic nanoparticles are suspended to improve the heat transfer of conventional fluids.

Heat fluxes from Modern electronic devices have increased significantly. For electronic component cooling, it is very important to manage heat fluxes. To dissipate heat fluxes conventional cooling systems (air cooling techniques) are inadequate. For many heat transfer applications, conventional techniques have been replaced by other cooling techniques. The dispersing solid particles into a base fluid (nanofluid) for heat transfer applications enhances heat transfer coefficients and thermal conductivity.

It is essential to create efficient and high-performing heat transfer fluids for heat industrial processes. Electronic components deteriorate, decreasing component performance and increasing component failures due to overheating. To create high-performing electronic systems the heat dissipation from their components must be efficiently controlled. The average electronic chip heat flux exceeds 150 (W/cm^2) [2]. Dissipating heat from electrical devices is an important factor in improving information technology (IT).

ADHAM [3] Carried out the investigation of refrigerant base nanofluid (Al_2O_3-NH_3) as a coolant for electronic chips. He concluded that using (Al_2O_3-NH_3) coolant will outperform other coolants like (SiC-H_2O, TiO_2-H_2O, H_2O and Al_2O_3-H_2O) in terms of pumping power demand by up to 85%. Adham et al. [4] carried out an analytical study on the thermal resistance and pressure drop of a microchannel heat sink with rectangular shape utilizing ammonia as a coolant. They concluded a significant thermal resistant reduction with 0.213 $^oK/W$ for ammonia gas when compared to that of 0.266 $^oK/W$ for air.

Sohel et al. [5] showed heat transfer improvements from the use of minichannel heat sinks electronic cooling with a Al_2O_3–H_2O nanofluid coolant for volume fractions from 0.1 – 0.25 %. The heat transfer coefficient was enhanced by 18%, heat sink base temperature was reduced by 2.7°C, and thermal resistance was reduced by 15.72%. Li and Xuan [6] investigated the convective heat transfer of CuO-H_2O base nanofluids in a tube. Their results showed that the use of nanofluids improved heat transfer rate compared to pure water.

Nguyen et al. [7] reported the thermal behavior of Al_2O_3–H_2O nanofluid as a microprocessor coolant. Their results indicated the enhancement of heat transfer coefficients by 40% compared to the base fluid. Lee et al. [8] presented that the thermal conductivity of CuO-ethylene glycol nanofluid with 4% particle volume concentration could be enhanced by up to 20%. Chen [9] analyzed forced convection heat transfer through microchannel heat sinks for electronic cooling systems. Gillot et al. [10] evaluated the use of single-phase and two-phase micro heat sinks to cool power components.

Chein and Huang [11] studied silicon microchannel heat sink performance using a CuO- H_2O nanofluid as a coolant. They indicated that heat sink performance has significantly enhanced by the nanofluid.

Ding et al. [12] investigated the heat transfer performance of CNT nanofluids flowing in a horizontal tube with an inner diameter of 4.5 mm. They were showed that increases in the heat transfer coefficient were much greater with increases in thermal conductivity.

The study aims analytically examines nanofluid thermal conductivity, heat transfer coefficient, flow rate, pumping power, and pressure drop for a rectangular copper minichannel heat sink that used CuO-H_2O and Graphite-H_2O as coolants. In addition, it investigates the effect of using appropriate equations to calculate the thermophysical properties of the nanofluids on the overall performance of the considered system.

2. Mathematical Model

2.1. Nanofluids

In this study, CuO nanoparticles and graphite nanoparticles suspended in water were mathematically analyzed. The thermophysical properties of CuO, Graphite and water at 30℃ were used [13]. Table 1 Lists the Thermophysical properties of the water and nanoparticles.

Table 1. Thermophysical properties of water and nanoparticles

Properties	Water	CuO	Graphite
ρ (kg/m^3)	995.8	6500	2490
μ (kg/m.s)	8.034x10^{-4}	----	----
Cp (J/kg.K)	4178.4	536	771
K (W/m.K)	0.617	20	114

The thermophysical properties of CuO-H_2O and Graphite-H_2O nanofluids were calculated using particle volume fractions of 1%, 2%, 3%, 4%, and 5%. The density [14], viscosity [15], specific heat, and thermal conductivity [16] were determined using Eq. (1) to (4):

$$\rho_{nf} = \left(1-\phi\right)\rho_f + \phi\rho_p \tag{1}$$

$$\mu_{nf} = \frac{1}{(1-\phi)^{2.5}}\mu_f \tag{2}$$

$$(\rho c_p)_{nf} = \frac{(1-\phi)(\rho c_p)_f + \phi(\rho c_p)_p}{\rho_{nf}} \tag{3}$$

$$\frac{k_{nf}}{k_f} = 1.0 + 1.0112\phi + 2.4375\phi\left(\frac{47}{n}\right) - 0.0248\phi\left(\frac{k_p}{0.613}\right) \tag{4}$$

Nanoparticles were assumed to be spherical particles with n=3

2.2. Minichannel Heat Sink

2.2.1. Heat Flux

This paper examined a copper minichannel heat sink. The dimensions of the copper minichannel heat sink were taken from Xie et al. [17] and are shown in Fig. 1.

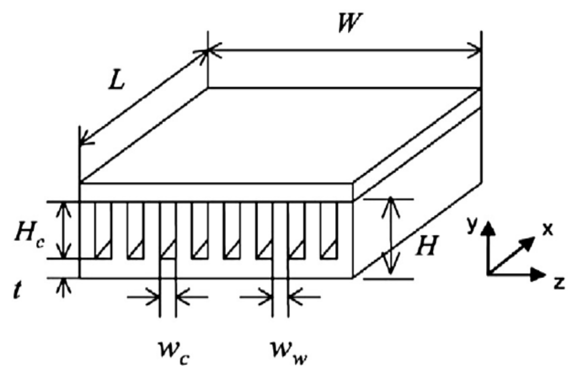

Figure 1. Schematic view of the microchannel heat sink model [19]

Assumptions:

The flow was laminar, incompressible, and steady state; the thermophysical properties of CuO-H_2O and graphite-H_2O were constant; and the effect of body force was neglected.

The nanofluid Reynolds number was defined as [13]:

$$\mathrm{Re} = \frac{V_m D_h}{\nu} \tag{5}$$

Hydraulic diameter was the ratio between channel cross-sectional areas and the perimeter [13], which was computed using Eq. (6):

$$D_h = \frac{4W_c H_c}{2(W_c + H_c)} \tag{6}$$

Where 0.1 m/s and 1.5 m/s are the mean velocities of CuO-H_2O and graphite-H_2O in the minichannel heat sink, respectively [17].

$$\mathrm{Pr} = \left(\frac{c_p \mu}{k}\right)_{nf} \tag{7}$$

Nusselt number was a dimensionless parameter defined as the ratio of convective to conductive heat transfer [13]. The Nusselt number for nanofluid laminar flow through a minichannel heat sink was calculated using Eq. (8) [18]:

$$Nu = 2.253 + 8.164\left(\frac{\alpha_s}{\alpha_s + 1}\right)^{1.5} \tag{8}$$

Where α_s is the channel aspect ratio

The convective heat transfer coefficient h was evaluated from the Nusselt number using Eq. (9):

$$h = \frac{Nu k_{nf}}{D_h} \tag{9}$$

The efficiency of copper MCHS was calculated using Eq. (10) and (11).

$$m \times H_c = \sqrt{\frac{2h}{k_s W_w}} \times H_c \tag{10}$$

η is fin efficiency, which was expressed as:

$$\eta = \frac{\tanh(m \times H_c)}{m \times H_c} \tag{11}$$

Surface area was written as:

$$A_{sf} = nW_c L + 2n\eta H_c L \tag{12}$$

where n is the number of cooling channels. There were 25 channels for the fixed width of the heat sink [17]. Total thermal resistance was the summation of three thermal resistances, calculated using Eq. (13) [20]:

$$Rt = \frac{1}{hA_{sf}} + \frac{1}{\dot{m} c_p} + \frac{H_b}{k_s A_{bm}} \tag{13}$$

where $\dot{m}$ is the total coolant mass flow rate through channel inlets and A_{bm} is the bottom area of a rectangular minichannel heat sink, which was calculated using Eq. (14) [13]:

$$\dot{m} = n\rho_{nf} A_c V_m \tag{14}$$

Overall thermal resistance Rt and temperature differences for heat generation rate Q were computed using Eq. (15):

$$Q = \frac{T_{\max} - T_{min}}{R_t} \tag{15}$$

$$\dot{q} = \frac{Q}{A_{bm}} \tag{16}$$

where $\dot{q}$ is heat flux, T_{max} is the maximum bottom temperature, T_{in} is inlet fluid temperature, and Q is total heat transfer. The highest temperature difference (T_{max} - T_{in}) was taken as 50°C [17]

2.2.2. Pressure Drop and Pumping Power

Heat sink pressure drop was obtained through the conservative Darcy friction factor as in Eq. (17) [21]:

$$\Delta P = f \frac{L}{D_h} \frac{\rho V_m^2}{2} \tag{17}$$

$$f = \frac{96(1 - 1.3553\alpha + 1.9467\alpha^2 - 1.7012\alpha^3 + 0.9564\alpha^4)}{\mathrm{Re}} \tag{18}$$

where α is the channel aspect ratio

Required pumping power was calculated using Eq. (19):

$$P_p = \dot{V}\Delta P \tag{19}$$

3. Result and Discussion

The results showed that the addition of graphite nanoparticles to the base fluid (water) had a significant effect on thermal conductivity. Fig. 2 shows variations in graphite-H_2O thermal conductivity with different particle volume fractions. The thermal conductivity of graphite-H_2O increased with increased particle volume fractions. The maximum thermal conductivity for graphite-water was about 0.7128 W/m.K at 5% particle volume fraction and the greatest enhancement in thermal conductivity was 15.52%. In addition, the thermal conductivity of CuO-H_2O nanofluid was improved through the addition of nanoparticles.

Figure 3 shows that the greatest improvement in thermal conductivity for CuO-H_2O with 5% volume concentration was 14.34%. Thermal conductivity was computed based on Hamilton and Crosser model (Eq. (4)). Liu et al. [22] measured the thermal conductivity of CuO-water with a 5% volume fraction. Their results showed that an improvement of thermal conductivity of around 22.4%. In this study, the effect of Brownian motion was neglected but the effect of particle volume fraction on thermal conductivity and particle shape was taken into account.

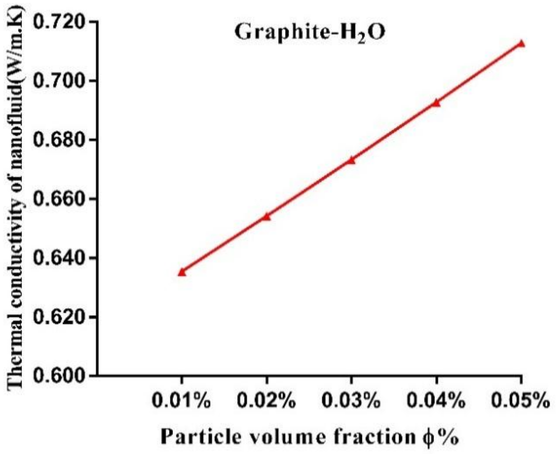

Figure 2. Thermal conductivity for Graphite-H_2O nanofluids versus particle volume fractions

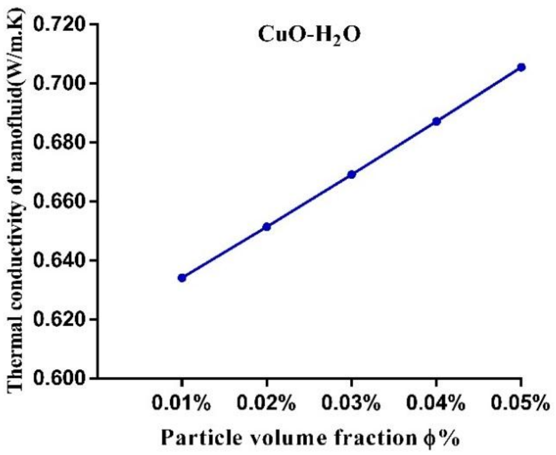

Figure 3. Thermal conductivity for CuO-H_2O nanofluids versus particle volume fractions

The measurement results show that nanofluid thermal resistance remarkably decreased with increased Reynolds numbers, while convective heat transfer coefficient increased. For inlet velocities of 0.1m/s and 1.5m/s for graphite-water and CuO-water nanofluids (Eq. (5) and (13)), thermal conductivity, heat transfer coefficient, and thermal resistance influenced each other. For example, the thermal conductivity of graphite-water nanofluid with 1% particle volume fraction was 0.6354 W/m. K with a 6533 W/m2.K heat transfer coefficient and an 0.0805 W/K thermal resistance. By increasing the particle volume fraction to 5% the heat transfer coefficient and thermal resistance changed to 7329W/m^2. K and 0.0781 K/W, respectively. The same results occurred for CuO-water at inlet velocities 0.1 m/s and 1.5 m/s as shown in Fig.4 and Fig.5.

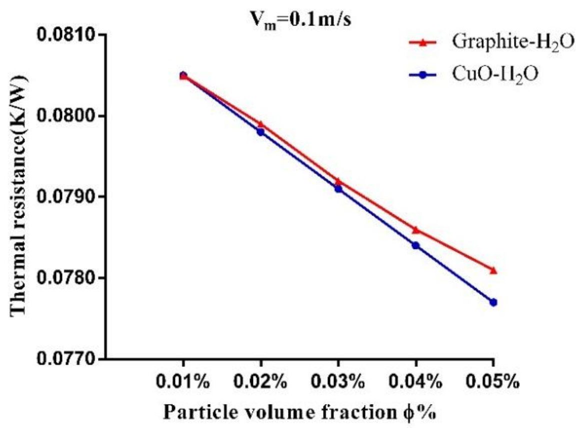

Figure 4. Thermal resistance at 0.1 m/s versus particle volume fractions

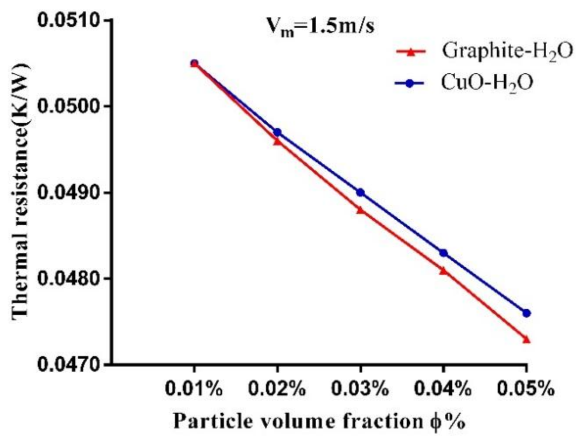

Figure 5. Thermal resistance at 1.5 m/s versus particle volume fractions

As expected, mass flow rate was directly proportional to the heat transfer coefficient for graphite-water and CuO-water, as mass flow rate increased with increased heat transfer coefficients (Eq. (14) and (9)). In addition, nanofluid density increased when increased particle volume fractions were added to the base fluid, which increased the convection heat transfer coefficient and inlet velocity for graphite-water and CuO-water. Nanofluid density was computed using Eq. (1). For instance, at 0.1m/s the density of CuO-water nanofluid has 1050.84kg/m^3 with 1% particle volume concentration and a mass flow rate equal to 0.0079 kg/s with a 6519 W/m^2. K convective heat transfer coefficient. At 5% volume fraction density was 1271.01 kg/m^3 with a mass flow rate of 0.0095kg/s and a volume fraction density of 7254 W/m^2. K as shown in Figs.

6 and 7.

Increased volume concentrations enhanced the heat flux of both nanofluids, which was calculated using Eq. (16). From this study it can be observed that the greatest improvement in heat flux with 1% particle volume concentration from the use of 0.1m/s graphite-water and CuO-water nanofluids were 17.83% and 18%, respectively, and 1.5m/s graphite-water and CuO-water was 3.33% and 3.46%, respectively, for both inlet velocities. For the CuO-water nanofluid the maximum enhancement in heat flux was 13.15% at 4% volume fraction while improvements from TiO_2-water and Al_2O_3-water were 6.20% and 6.80%, respectively. The thermal conductivity of nanoparticles is higher than the base fluid (water). Thus, the addition of nanoparticles to the base fluid led increases its convective heat transfer coefficient, thermal conductivity, and heat flux while decreasing thermal resistance as shown in Fig.8 and Fig. 9.

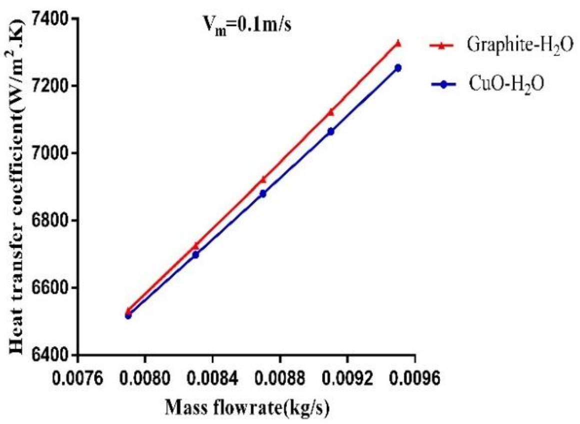

Figure 6. Heat transfer coefficient at 0.1 m/s versus mass flowrate

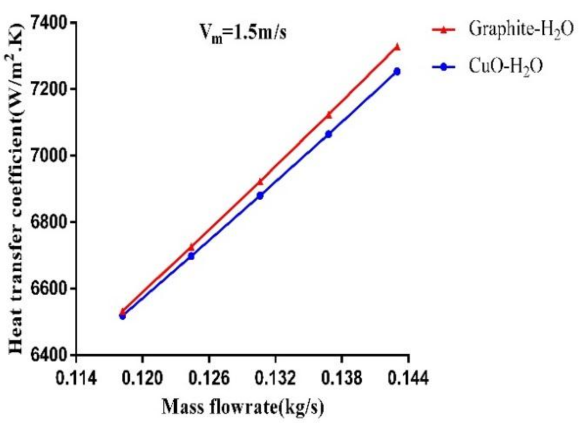

Figure 7. Heat transfer coefficient at 1.5 m/s versus mass flowrate

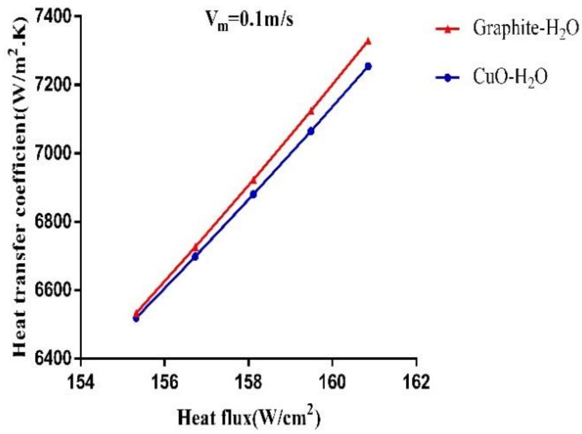

Figure 8. Heat transfer coefficient at 0.1 m/s versus heat flux

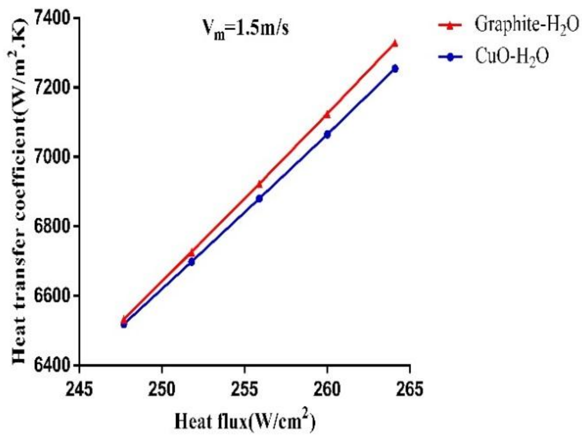

Figure 9. Heat transfer coefficient at 1.5 m/s versus heat flux

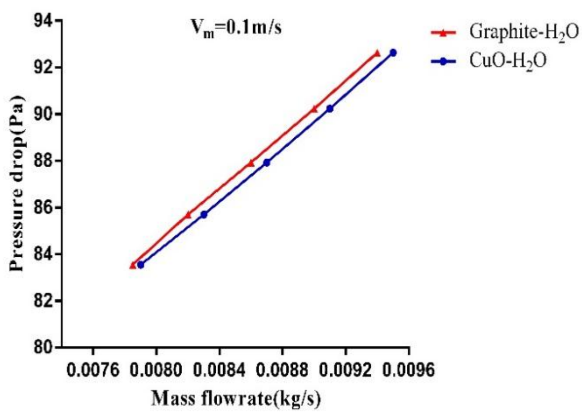

Figure 10. Pressure drop at 0.1 m/s versus mass flowrate

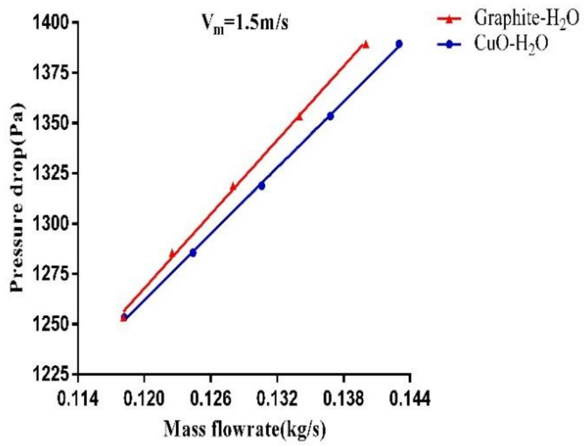

Figure 11. Pressure drop at 1.5 m/s versus mass flow rate

An important parameter for minichannel heat sinks is pressure drop. Pressure drop linearly increased with increased mass flow rates for both graphite-water and CuO-water nanofluids, which was computed using Eq. (17). Pressure drop is a function of inlet velocity and nanofluid density. For instance, at 0.1m/s inlet velocity with 1% concentration, the pressure drop for graphite-water nanofluid was 83.55 Pa with 1010.74 kg/m^3 density. On the other hand, at 5% volume fraction concentration the pressure drop was 92.63 Pa and the density was equal to 1070.51 kg/m^3 as shown in Fig. 10 and Fig. 11

Xie et al[17] studied a minichannel heat sink similar to the one used in this study. Their results showed that at 0.1m/s pressure drop was 70Pa with 5.3*10-4 W pumping power, and at 1.5m/s inlet velocity the pressure drop and pumping power were 1817 Pa and 0.205 W, respectively. At 0.1m/s with 1% vol. and 5% vol. the pumping power of the graphite-water and CuO-water nanofluids were 0.000627 W and 0.000695 W, respectively. The pumping power for both nanofluids at 1.5m/s with 1% and 5% of particles volume fractions were 0.140993 W and 0.156306 W, respectively. Pressure drop is related to pumping power, as when pressure drop increased pumping power increased for graphite-water and CuO-water nanofluids with 0.1 m/s and 1.5 m/s inlet velocities as shown in Figs. 12, 13, 14, and 15.

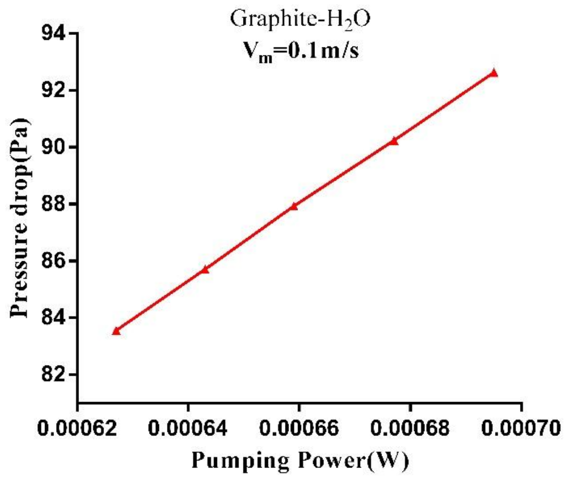

Figure 12. Pressure drop at 0.1 m/s versus pumping power

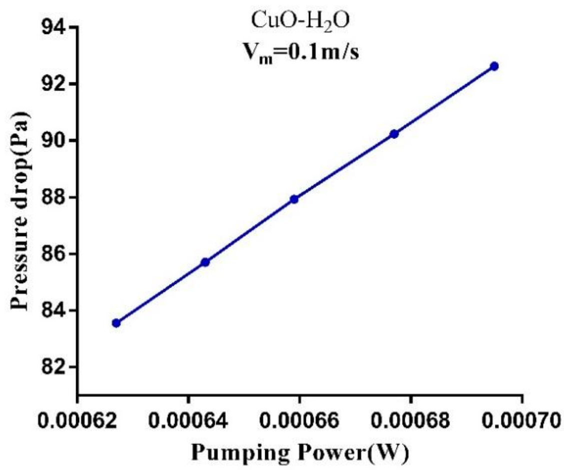

Figure 13. Pressure drop at 0.1 m/s versus pumping power

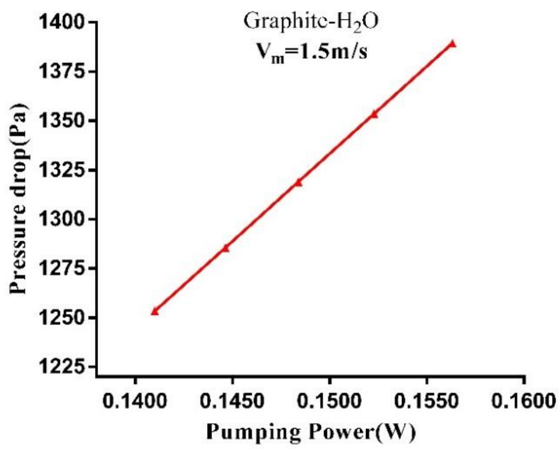

Figure 14. Pressure drop at 1.5 m/s versus pumping power

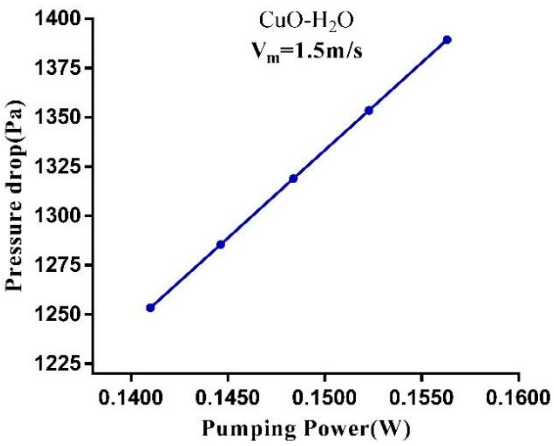

Figure 15. Pressure drop at 1.5 m/s versus pumping power

For graphite-water and CuO-water nanofluids increases in the particle volume fraction present in the base fluid (water) increased thermal conductivity and convective heat transfer coefficient, which increased pumping power as pumping power linearly increases with increased heat transfer coefficients. Pumping power was computed using Eq. (19).

4. Conclusions

In summary, this paper investigated nanofluid thermal conductivity, heat flux, and pumping power. Two particular nanofluids, namely Graphite-H_2O and CuO-H_2O, were studied as coolants. The results illustrated that the dispersion of nanoparticles into the base liquid led to an increase in thermal conductivity. For graphite-H_2O and CuO-H_2O at 5% particle volume concentration, the greatest improvement in thermal conductivity was 15.52% and 14.34%, respectively. Significant improvements were observed for nanofluid thermal conductivity in comparison to pure water.

The maximum enhancement of heat flux from the use of graphite-H_2O with 1% volume fraction at 0.1 m/s was 18% greater than the base fluid. At 1.5 m /s inlet velocity with the same volume concentration, the maximum rise heat flux was 3.46%. For CuO-H_2O nanofluids at 0.1 m/s and 1.5 m/s inlet velocity with a volume fraction of 1% volume, heat flux was enhanced by 17.83% and 3.33%, respectively. It was found that the maximum pumping power and pressure drop from the use of graphite-H_2O and CuO-H_2O at 0.1 m/s inlet velocity with 5% volume fraction were 0.000695 W and 92.63 Pa, respectively. On the other hand, at 1.5 m/s the maximum increase in pumping power and pressure drop for both nanofluids were 0.156306 W and 1389.39 Pa, respectively for 5% nanofluid volume fraction.

Nomenclature

A_{bm} Bottom area of minichannel heat sink (m^2)
A_c Channel area (m^2)
A_{sf} Surface area available for heat transfer (m^2)
c_p Specific heat (J/kg.K)
D_h Hydraulic diameter of the fluid flow (m)
f Friction factor
H_b Bottom plate thickness (m)
H_c Channel height (m)
h Heat transfer coefficient (W/m^2.K)
k_{nf} Thermal conductivity of nanofluid (W/m.K)
k_f Thermal conductivity of fluid (W/m.K)
k_s Thermal conductivity of heat sink (W/m.K)
Re Reynolds number
Rt Total thermal resistance (K/W)
T_{max} Maximum temperature (K)
T_{min} Minimum temperature (K)
V_m Inlet velocity (m/s)
$\dot{V}$ Volumetric flow rate (m^3)
W_c Channel Width (m)
W_w Channel wall thickness (m)
ΔP Pressure drop (kPa)

Greek Symbols

μ Dynamic viscosity (kg/m.s)
Ø Particle volume fraction
L Channel length (m)
$\dot{m}$ Total coolant mass flow rate (kg/s)
Nu Nusselt number
n Number of cooling channels
P_p Pumping power (W)
Pr Prandtl number
P Pressure (kPa)
Q Heat generation (W)
$\dot{q}$ Heat flux (W/cm^2)
η Fin efficiency
ρ Density (kg/m^3)
v Kinematic viscosity of fluid (m^2/s)
α Channel aspect ratio

REFERENCES

[1] W. Yu, D. M. France, S. U. Choi, J. L. Routbort, Review and Assessment of Nanofluid Technology for Transportation and other Applications, Argonne National Laboratory (ANL), 2007.

[2] A. Bar-Cohen, M. Arik, and M. Ohadi, Direct Liquid Cooling of High Flux Micro and Nano Electronic Components, Proceedings of the IEEE, Vol. 94, n. 8, pp. 1549-1570, 2006.

[3] A. M. ADHAM, Amonia Base Nanofluid as a Coolant for Electronic Chips, International Joural of Mechanical and Production Enginnering Research and Development, Vol. 9, n. 3, pp. 569-579, 2019.

[4] A. M. Adham, N. Mohd-Ghazali, R. Ahmad, Thermal

Performance of Ammonia-Cooled Microchanel Heat Sink, International Journal of Mechanical Engineering, Vol. 6, n. 4, pp. 828-836, 2012.

[5] M. Sohel, S. Khaleduzzaman, R. Saidur, A. Hepbasli, M. Sabri, I. Mahbubul, An Experimental Investigation of Heat Transfer Enhancement of a Minichannel Heat Sink Using Al 2 O 3–H 2 O Nanofluid, International Journal of Heat and Mass Transfer, Vol. 74, pp. 164-172, 2014.

[6] Q. Li, Y. Xuan, J. Wang, Investigation on Convective Heat Transfer and Flow Features of Nanofluids, Journal of Heat transfer, Vol. 125, n. 1, pp. 151-155, 2003.

[7] C. T. Nguyen, G. Roy, C. Gauthier, N. Galanis, Heat Transfer Enhancement Using Al 2 O 3–Water Nanofluid for an Electronic Liquid Cooling System," Applied Thermal Engineering, Vol. 27, n. 8-9, pp. 1501-1506, 2007.

[8] S. Lee, S.-S. Choi, S. Li, J. Eastman, Measuring Thermal Conductivity of Fluids Containing Oxide Nanoparticles, Journal of Heat transfer, Vol. 121, n.2, pp. 280-289, 1999.

[9] C.-H. Chen, Forced Convection Heat Transfer in Microchannel Heat Sinks, International Journal of Heat and Mass Transfer, Vol. 50, n. 11-12, pp. 2182-2189, 2007.

[10] C. Gillot, A. Bricard, C. Schaeffer, Single-and Two-Phase Heat Exchangers for Power Electronic Components, International journal of thermal sciences, Vol. 39, n. 8, pp. 826-832, 2000.

[11] R. Chein, G. Huang, Analysis of Microchannel Heat Sink Performance Using Nanofluids, Applied Thermal Engineering, Vol. 25, n. 17-18, pp. 3104-3114, 2005.

[12] Y. Ding, H. Alias, D. Wen, R. A. Williams, Heat Transfer of Aqueous Suspensions of Carbon Nanotubes (CNT Nanofluids), International Journal of Heat and Mass Transfer, Vol. 49, n. 1-2, pp. 240-250, 2006.

[13] T. L. Bergman, A. S. Lavine, F. P. Incropera, D. P. Dewitt, Fundamentals of heat and mass transfer (7th edition, Wiley, 2011)

[14] D. A. Drew, S. L. Passman, Theory of Multicomponent Fluids, (1st edition, Springer, 1999).

[15] S. Q. Zhou, R. Ni, Measurement of the specific heat capacity of water-based Al2O3 nanofluid," Appl. Phys. Lett. 92, 093123, 2008.

[16] K. Khanafer, K. Vafai, A critical synthesis of thermophysical characteristics of nanofluids, International Journal of Heat and Mass Transfer, Vol. 54, pp. 4410-4428, 2011.

[17] X. Xie, Z. Liu, Y. He, W. Tao, Numerical Study of Laminar Heat Transfer and Pressure Drop Characteristics in a Water-Cooled Minichannel Heat Sink, Applied Thermal Engineering, Vol. 29, n. 1, pp. 64-74, 2009.

[18] S. Kim, D. Kim, Forced Convection in Microstructures for Electronic Equipment Cooling, Transactions-American Society of Mechanical Engineers Journal of Heat Transfer, Vol. 121, n. 3, pp. 635-645, 1999.

[19] S. Halelfadl, A. M. Adham, N. Mohd-Ghazali, T. Maré, P. Estellé, R. Ahmad, Optimization of Thermal Performances and Pressure Drop of Rectangular Microchannel Heat Sink Using Aqueous Carbon Nanotubes Based Nanofluid, Applied Thermal Engineering, Vol. 62, pp. 492-499, 2014.

[20] R. W. Knight, D. J. Hall, J. S. Goodling, R. C. Jaeger, "Heat Sink Optimization with Application to Microchannels," IEEE Transactions on Components, Hybrids, and Manufacturing Technology, Vol. 15, n. 5, pp. 832-842, 1992.

[21] J. P. Hartnett and M. Kostic, Heat transfer to Newtonian and Non-Newtonian Fluids in Rectangular Ducts, Advances in heat transfer, Vol. 19, pp. 247-356, 1989.

[22] M. S. Liu, M. C. Lin, I. T. Huang, C. C. Wang, Enhancement of Thermal Conductivity with Cuo for Nanofluids, Chemical engineering & technology, Vol. 29, n. 1, pp. 72-77, 2006.